AEOLIAN BEDFORM GRAIN PROPERTIES AT GALE CRATER FROM VERA RUBIN RIDGE TO THE SANDS OF FORVIE. C. M. Weitz[1], R. J. Sullivan[2], M. Baker[3], and J. A. Grant[3]. [1]Planetary Science Institute, 1700 E. Fort Lowell, Tucson AZ 85719 (weitz@psi.edu) [2]Cornell University, Ithaca, NY 14853; [3]Smithsonian Institution, Washington DC, 20560;

Introduction: The physical properties of grains on aeolian bedforms can provide insight into sand transport and wind activity under current or past environmental conditions. In situ observations of grains on bedforms as seen from the surface are useful for providing ground truth for the ubiquitous aeolian bedforms observed in orbital images. In order to explore how grain properties vary as a function of parameters like bedform size, active vs inactive bedforms, and location on the bedform, we used Curiosity's Mars Hand Lens Imager (MAHLI) [1] to measure the size and shape of grains on aeolian bedforms at several locations within Gale Crater from when the rover was at Vera Rubin Ridge (VRR) to its current location (sol 29XX) at the Sands of Forvie (Fig. 1). These new measurements complement our previous analysis of aeolian bedforms made prior to arrival at the VRR [2].

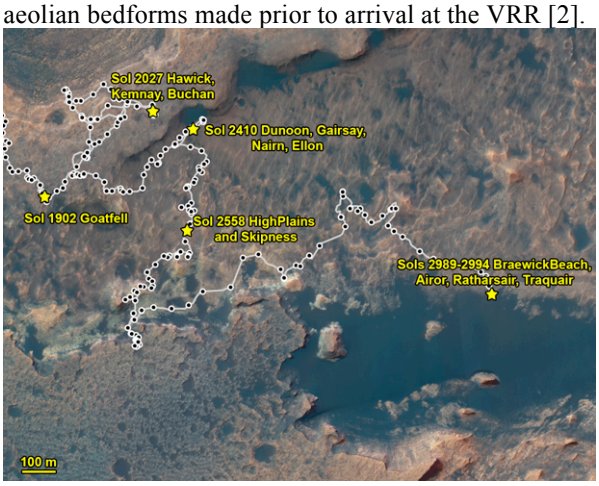

Figure 1. HiRISE color showing the Curiosity traverse (white) with the bedform target locations labeled.

Target Locations: The targets Goatfell (Sol 1902) and Hawick, Kemnay, and Buchan (Sol 2025) are in small ripple fields on the VRR (Fig. 1). Targets Dunoon, Gairsay, Nairn, and Ellon were acquired on Sol 2410 within a large ripple field adjacent to the VRR (Fig. 1). Targets High Plains and Skipness (Sol 2558) were on the crest and flank, respectively, of a bright isolated TAR-like (Transverse Aeolian Ripple) bedform called Culbin Sands 2. Lastly, the rover acquired targets Braewick_Beach, Airor, Ratharsair, and Traquir at the Sands of Forvie sand sheet between Sols 2989-2994 (Fig. 1).

Analysis: Grain sizes were measured using the same procedure detailed in [2] where the length of the longest axis for each grain particle was measured. The occurrence of grains 50-100 µm in size or finer is likely underestimated, as their edges were not always clearly identifiable, especially at resolutions poorer than 20 µm. The aspect ratio for 100 grains larger than 150 µm in length, and where the entire grain shape was unobscured, were calculated after their shapes were outlined in ImageJ. Based upon observations of multiple MAHLI, Mastcam, and/or MARDI images as well as APXS data that show low values of S, Cl, and Zn for active sands [3], all targets locations except High Plains and Skipness are interpreted as currently active.

Results: Volume- or mass-based sieved size-fractions commonly used on Earth are not available from fundamentally two-dimensional Mars image data, and attempts to project a 3rd dimension down through bedforms imaged only at the surface are too dependent on 3-D regolith model assumptions that are highly uncertain. Instead, as in previous work, we present results conservatively in terms of simple grain size abundances at surfaces actually observed in the images. Figure 2 compares grains <600 µm in length from each of twelve MAHLI aeolian surface targets, indicating 50-

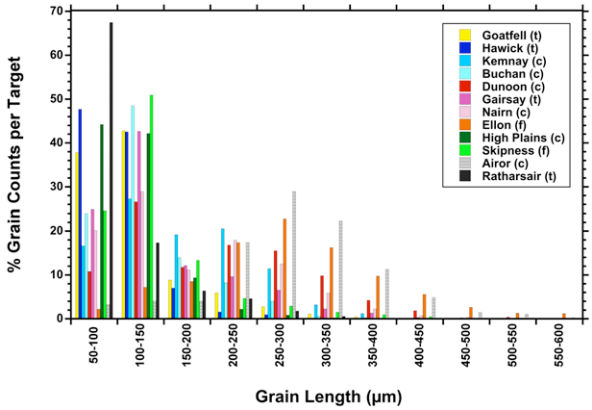

Figure 2. Grain size measurements for twelve MAHLI targets, excluding grains >600 µm, (c)=ripple crest, (t)=ripple trough, (f)=flank of ripple.

150 µm grains dominate, similar to results obtained elsewhere along the MSL traverse and at other Mars rover sites [2,4-7]. All grains >150 µm at these recent targets have some elongation with aspect ratios between 1.18-1.30. Targets Goatfell, Hawick, and Buchan have similar grain sizes and shapes with sands dominated by the 50-150 µm sizes. Coarser 150-1100 µm grains are present but in smaller amounts. Target Kemnay was located at the triple juncture of three ripple crests and the larger number of coarser grains at

this target compared to Hawick and Buchan taken at this same sandy location reflects the coarsening of grains along the relatively larger (cm-high) ripple crests.

MAHLI images were acquired on sol 2410 at four different targets at the Rigg ripple field site (Figs. 1,3). Dunoon is located along a larger ripple crest that is dominated by 100-150 µm grains with a significant population of coarser mm-size grains (Fig. 3). Gairsay was in a ripple trough and it is dominated by the smaller 50-150 µm grains. Nairn was on a smaller ripple crest relative to the Dunoon target. It has a similar size distribution to Dunoon, except it lacks the mm-size granules observed along the larger Dunoon ripple. Finally, target Ellon was on the lee side flank of the same ripple as Dunoon. Coarser >200 µm size grains collected along the ripple flank where there was a change in slope from steeper to shallower (Fig. 3). The largest grains on the ripple (2-3 mm) are rough, elongate, and either red or white in color, indicating they are derived from erosion of the local bedrock.

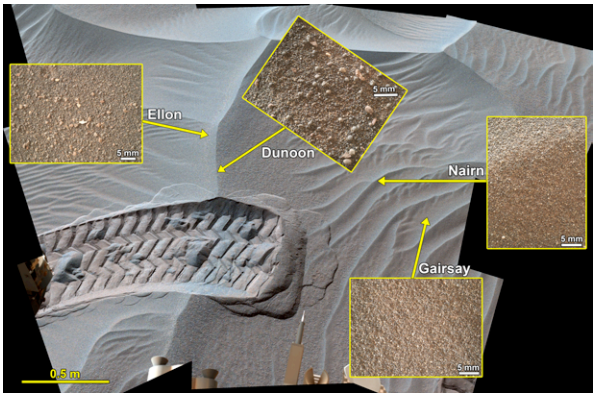

Figure 3. Mastcam mosaic of the Rigg ripple field with approximate locations of the MAHLI images (arrows). Rover wheel scuff is shown in foreground.

The surface of the bright TAR-like bedform at Culbin Sands 2 is armored by coarser grains (Fig. 4), similar to what was observed at the inactive bright Rocknest (sol 58) and Barker (sol 531) bedforms [2,9] and may be analogous to desert pavements on Earth. The bedform flanks have fewer of the mm-size granules and pebbles relative to the bedform crest. The grains appear smooth and well-rounded, indicating they have been eroded by the wind for an extended period of time. Unlike the active bedforms which have a large percentage of darker basaltic sands, the coarser grains on the TAR-like bedform are redder and presumed to be derived from the local bedrock. Targets High Plains and Skipness located on this bedform are dominated by the 50-150 µm sizes in between coarser grains (0.3-11 mm) along the surface. MAHLI images show grains are coated with dust aggregates and the interior of the bedform exposed within the wheel scuff exhibits cohesion along the surface, consistent with the bedform being inactive. Due to the lower resolution of the MAHLI images and clumping of the soil, we were not able to measure individual grain sizes exposed within the bedform interior by the wheel scuff. Nevertheless, we visually estimate from these images that the interior is dominated by finer sands with a smaller population of mm-size granules.

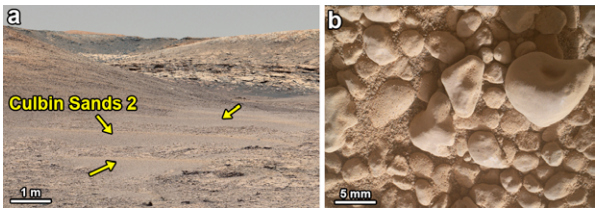

Figure 4. (a) Mastcam mosaic showing three bright TAR-like bedforms (arrows), including location Culbin Sands 2 where the MAHLI images were taken. (b) MAHLI image of target High Plains taken along the crest of the Culbin Sands 2 bedform. Note the bright dust coating all the grains.

At the Sands of Forvie sand sheet, four MAHLI targets were acquired (Fig. 1). Target Braewick_Beach was taken along the stoss flank of a large transverse ripple crest. A rover wheel was then used to scuff a large ripple just to the east where the other three targets were acquired, including Airor on a large transverse ripple crest, Ratharsair in the ripple trough, and Traquair on a smaller secondary ripple crest. Similar to what was observed at Rigg, the crest and flank surfaces of the larger ripples had coarsening of grains compared to the troughs and smaller secondary ripples.

Conclusions: New grain size measurements from recent aeolian stops along the MSL traverse are consistent with previous measurements at Gale [2,4-6] showing sand grains 50-150 µm in size are abundant on and within active aeolian bedforms. Coarser grains 150-500 µm can be significant along surfaces of crests and flanks of larger bedforms, which also have smaller numbers of even coarser 1-3 mm grains. Granule and pebble sizes that are small rock fragments eroded from the local bedrock armor inactive bedforms.

References: [1] Edgett, K.S. et al., (2012) *Space Sci. Rev., 170*, 259-317. [2] Weitz C.M. et al. (2018) *Geophys. Res. Letts. 45*, 9471-9479; [3] O'Connell-Cooper C.D. et al. (2018) *Geophys. Res. Letts. 45*, 9460-9470; [4] Ewing, R.M. et al (2017) *J. Geophys. Res., 122*, 2544-2573; [5] Ehlmann, B.K. (2017) *J. Geophys. Res*., 122(12), 2510-2543; [6] Lapotre, M. et al. (2018) *Geophys. Res. Letts. 45*, 10229-10239; [7] Jerolmack, D.J. et al. (2006) *J. Geophys. Res., 111*, E12S02; [8] Sullivan, R., et al. (2008) *J. Geophys. Res., 113,* E06S07*;* [9] Minitti, M.E. (2013), *J. Geophys. Res., 118(11),* 2338-2360.

Acknowledgements: We thank the MAHLI team for their efforts acquiring these images.